THE PROTEIN SOCIETY

In silico study of human aquaporin AQP11 and AQP12 channels

Luisa Calvanese,[1] Marialuisa Pellegrini-Calace,[2] and Romina Oliva[1]*

[1]Department of Applied Sciences, University Parthenope of Naples, Centro Direzionale Isola C4, Naples I-80143, Italy
[2]Network of Public Research Laboratories WAFITECH, Department of Biosciences, Biotechnologies and Pharmacological Sciences, University of Bari, Via Amendola 165/A, Bari 70126, Italy

Received 10 October 2012; Revised 3 January 2013; Accepted 21 January 2013
DOI: 10.1002/pro.2227
Published online 29 January 2013 proteinscience.org

Abstract: AQP11 and AQP12 are the most distantly related paralogs of the aquaporin family in human. They share indeed a low sequence similarity with other aquaporins and exhibit a modified N-terminal NPA signature motif. Furthermore, they have an anomalous subcellular localization. The AQP11 and AQP12 biological role remains to be fully clarified and their ability to allow transport of water is still debated. We have built accurate 3D-models for AQP11 and AQP12 and comprehensively compared their sequence and structure to other known aquaporins. In order to investigate whether they appear compatible or not with water permeability, we especially focused on the amino acid composition and electrostatics of their channels, keeping the structure of the low-water efficiency AQP0 as a reference system. Our analysis points out a possible alternative ar/R site and shows that these aquaporins feature unique residues at key pore-lining positions that make the shape, composition and electrostatics of their channel peculiar. Such residues can represent pivotal hints to study and explain the AQP11 and AQP12 biological and molecular function.

Keywords: aquaporins; water transport; electrostatics; pore analysis; molecular modeling

Introduction

Aquaporins (AQPs) represent a family of transmembrane channel proteins, which allow osmotic-driven transport of water and small solutes across biological membranes and are found in all living organisms, with only few exceptions. According to their specific transport selectivity and efficiency, source, localization, and physiological function, aquaporins have been grouped by phylogenetic analyses into about 30 major subfamilies.[1] These subfamilies can be further classified into two major families: orthodox aquaporins, which only transport water, and aquaglyceroporins, which preferentially allow the transport of small organic compounds like glycerol and urea.

Many biochemical and structural studies have demonstrated that, despite a very variable sequence similarity, AQP subfamilies share the same structural architecture.[2,3] In particular, AQPs are homo-oligomers of four functional monomers. Each monomer is a right-handed bundle of six transmembrane and two re-entrant half-spanning helices, which shape a central hourglass-like channel. Each monomer also shows: (1) two conserved Asn-Pro-Ala (NPA) sequence motifs, which cap the end of the two half helices and lie at the middle of the permeation channel, where they form a constriction; (2) another narrower constriction, known as aromatic/Arg (ar/R) selectivity filter, which is located at the periplasmic side of the channel and is formed by four residues, including a strictly conserved arginine and an aromatic residue, such as Phe or Trp. The ar/R filter is the most significant and conserved difference between aquaporin and aquaglyceroporin channels,

Additional Supporting Information may be found in the online version of this article.

Grant sponsor: MIUR PON-SPACI 2006; Grant number: 68/2002.

*Correspondence to: Romina Oliva, Department of Applied Sciences, University of Naples Parthenope, Centro Direzionale Isola C4, I-80143, Naples, Italy. E-mail: romina.oliva@uniparthenope.it

in terms of sequence and consequently structure and selectivity.[4]

The number of aquaporin subfamilies per species is very variable. Thirteen AQPs have been identified in human (AQP0–12), of which AQP3, 7, 9, and 10 are aquaglyceroporins and AQP11 and 12 are the most distantly related paralogs, with fairly low amino acid sequence identity with the remaining family members.[5] Notably, AQP11 and AQP12 show the N-terminal NPA modified into Asn-Pro-Cys (NPC) and Asn-Pro-Thr (NPT), respectively.[5] In addition, they localize on the membrane of intracellular organelles instead of the plasma membrane. AQP11 and AQP12, both on the basis of sequence and localization features, are therefore hardly classifiable as either orthodox aquaporins or aquaglyceroporins and have been proposed as a third aquaporin group, the superaquaporins[6] or subcellular aquaporins,[7] according to their cellular localization.

AQP12 is exclusively found in pancreatic acinar cells[8] and is therefore possibly involved in the secretion of digestive enzymes and fluids in the pancreatic cells. Interestingly AQP12 genes can also be found in *Caenorhabditis elegans* and in several vertebrates, including rat and chicken. Recently, a knockout (KO) mouse for this gene has been shown to be normal in terms of growth, blood chemistry, pancreatic fluid content, and histology. However, upon artificial induction of pancreatitis, it presented increased pathological damage when compared to the wild-type (WT).[9] The AQP12 water permeability was also investigated by using vesicles from the AQP12-KO and WT mouse pancreas, highlighting only a small non significant difference (of 1.9×10^{-3} cm/s) in the osmotic water permeability.[9]

AQP11 is to some extent more characterized.[3,7,10–15] It is expressed in many organs, such as testis, liver, brain, kidney, and heart, testis having the highest expression, and is particularly rich in cysteines. It has been suggested that AQP11 could work as a sort of intracellular aquaporin in certain tissues and have a role in intravesicular homeostasis of kidney proximal tubule cells, mammalian spermatogenesis and kidney, and salivary gland development.[12]

AQP11-KO mice have been shown to die before weaning due to polycystic kidney disease.[10] Interestingly, the single mutation to serine of a cysteine located nine residues downstream of the C-terminal NPA motif, that is conserved among putative members of the third AQP group, while not found in either orthodox AQPs or aquaglyceroporins, has also been shown to produce a phenotype similar to that of AQP11-null mice, suggesting that the residue is needed for AQP11 to function.[15] As for its transport properties, the water permeability of AQP11 is controversial, as it was reported that AQP11 expressed on Xenopus oocytes had no water permeability,[11] whereas stopped-flow light scattering experiments using reconstituted AQP11 on proteoliposomes revealed normal water permeability.[7] Nevertheless, a recent study showed that vesicles incorporating AQP11 directly formed from Sf9 cell membranes had appreciable water permeability (about one order of magnitude lower than that of AQP1) and were reversibly inhibited by mercury ions.[13] A comparative 3D model has also been obtained for hAQP11 by homology, starting from the crystallographic structure of the 18% sequence identical sheep AQP0,[16] an aquaporin with low transport efficiency. On the basis of such model, it was suggested that the slow water conduction of AQP11 could be due to a tyrosine residue (Tyr83) considered spatially corresponding to AQP0 Tyr149, which faces the channel pore and has been related to the AQP0 decreased water conduction rate.[13]

Herein, we present a structural bioinformatics study aimed at elucidating some of the structure-function relationships of the superaquaporins AQP11 and AQP12. Indeed, nowadays the variety of available aquaporin 3D-structures represent a valuable resource to identify sequence, structural, and physico-chemical features, which correlate to diverse transport selectivities within this protein family. We have performed a comprehensive analysis of the AQP11 and AQP12 channels and compared them with all other known aquaporins, both in terms of sequence and, when possible, structure. To this aim, we combined multitemplate comparative modeling techniques with novel computational methods specifically designed for the structural analysis and characterization of the pore of integral membrane proteins.[17–19] In particular, we extracted amino acids at the pore-lining positions and visualized them by means of pore-logo representations, which give an effective and immediate view of the pore residue composition.[18] Then, we calculated channel electrostatic profiles for *in silico* generated site-specific mutants, as channel electrostatics has revealed to be a key feature to discriminate between aquaporins with different selectivities.[17,20] In particular, we have previously shown that the channel of AQP1 and other orthodox aquaporins has an electrostatic profile characterized by a fairly flat area in the cytoplasmic half and a strong positive trend in the periplasmic half, with a peak at the ar/R constriction site. This may provide a driving force to the water molecules to cross the channel. Water molecules have indeed been shown by molecular dynamics to cross aquaporins oriented in opposite directions in the two halves of the channels, with oxygen atoms pointing toward the center.[21,22] The channel of bovine AQP0 (BtAQP0) also shows a strong positive trend in the periplasmic half, similarly to orthodox aquaporins, but presents an unusual trend, with negative values reaching a deep minimum in the cytoplasmic half. This characteristic profile may also be functionally significant, as

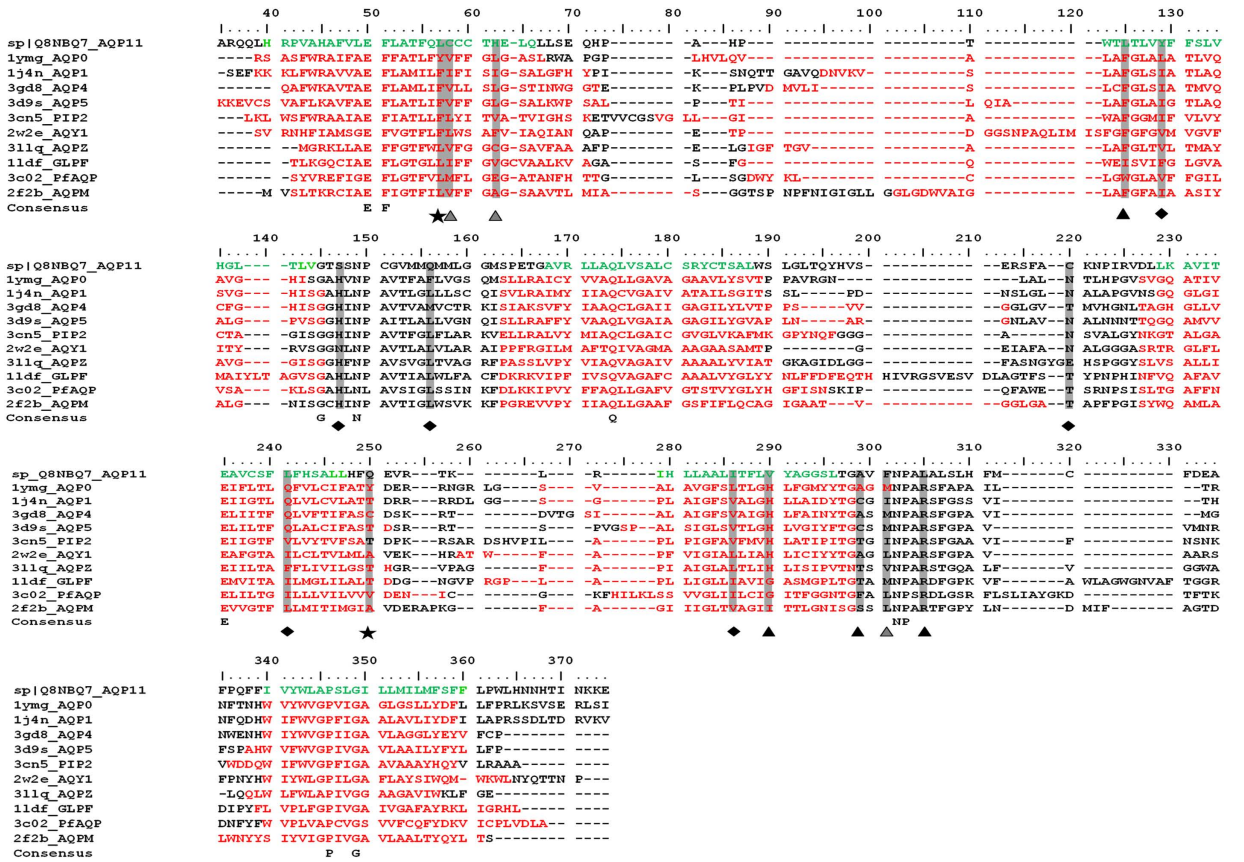

Figure 1. Multiple target-template alignment for human AQP11. hAQP11 residues predicted to be in trans-membrane helices by MEMSAT-SVM are colored green; residues assuming an helix conformation in the templates are colored red. Residues of the Ar/R selectivity filter and of the possible alternative Ar/R site are indicated with ▲ and ▲, respectively. Residues corresponding to the BtAQP0 sequence positions 23 and 149 are marked with ★. Other key pore-lining positions are pointed out with ◆. [Color figure can be viewed in the online issue, which is available at wileyonlinelibrary.com.]

it may cause the water molecules to reside longer in a stable configuration at the middle of the AQP0 channel. Therefore, the ability to restore an orthodox-like electrostatic profile of AQP11/AQP12-like mutants obtained from the structure of BtAQP0 has been investigated here. The effect of a given amino acid substitution was modeled by inserting it in the high resolution BtAQP0 structure, as the Poisson–Boltzmann calculations are also sensitive to the coordinates of peripheral regions, that are necessarily inaccurate in predicted 3D models. This follows an approach that we have previously demonstrated to be very effective.[17,20]

Our results show that AQP11 and AQP12, besides sharing significantly low sequence similarity with all other aquaporins, feature unique residues at key pore-lining positions that make their channel peculiar and could consequently represent pivotal hints to study and explain their biological and molecular function.

Results and Discussion

In the following, the 3D-models of hAQP11 and hAQP11 and the corresponding target-to-templates alignments (Figs. 1, 2 and 3) are presented and discussed. The amino acids lining the pore walls of hAQP11 and hAQP12 are also visualized using pore-logo representations [Fig. 3(b)] and compared with those of other mammalian aquaporins, and especially to AQP0 and AQP1 as prototypes of low-water conductance and orthodox aquaporins, respectively. Pore-logos give an effective and immediate view of the pore residue composition as they show contiguous amino acids, which are not necessarily adjacent in the sequence but lie spatially close in the channel.[18]

Pore-lining positions corresponding to the ar/R site and those hosting amino acids significantly different from other aquaporins for their size and/or physico-chemical properties are reported in Table I. They have been visualized in the 3D-models [Fig. 3(a)] and compared across all the aquaporins of known sequence. They are also outlined in the corresponding pore logo representations [Fig. 3(b)]. The available 10 3D-structures representative of different aquaporin subfamilies, including mammalian, plant, and bacterial aquaporins, have been comparatively analyzed, by keeping the structure of the low-water efficiency bovine AQP0 (BtAQP0, PDB code 1ymg) as reference system.

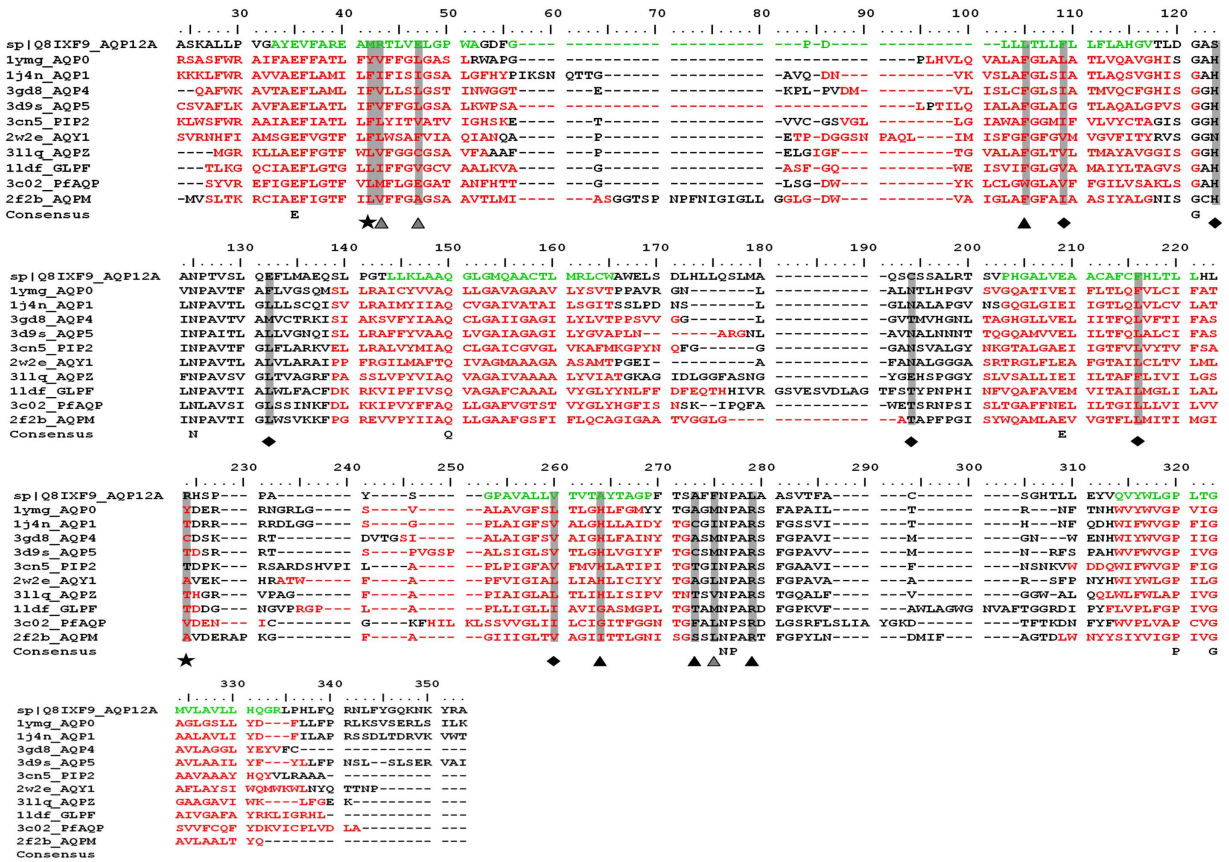

Figure 2. Multiple target-template alignment for human AQP12. hAQP12 residues predicted to be in trans-membrane helices by MEMSAT-SVM are colored green; residues assuming an helix conformation in the templates are colored red. Symbols are the same of Table I and Fig. 1. [Color figure can be viewed in the online issue, which is available at wileyonlinelibrary.com.]

Channel electrostatic profiles of *in silico* site-specific mutants, obtained by inserting key hAQP11/hAQP12 residues in the corresponding position of the BtAQP0 structure, are also presented. The channel electrostatics of aquaporins has indeed revealed to be a key feature to discriminate between different selectivities.[17,20] In Figure 4, the electrostatic profiles obtained for AQP11-like and AQP12-like mutants, at either the cytoplasmic or periplasmic side of the channel, are reported in separate panels. In the same figure, the channel electrostatic profiles of BtAQP0 and BtAQP1, already reported in Ref. 17 are also shown for the sake of comparison.

3D-models

3D-models of human AQP11 and AQP12 have been built by comparative modeling techniques. Considering the low sequence identity of AQP11 and AQP12 with aquaporins of known structure, a multitemplate approach has been adopted to extend the coverage.[23] To improve the quality of the target-templates alignments, reported in Figures 1 and 2, state-of-the-art procedures based on the comparison of profile hidden Markov models (HMMs)[24] have been combined with high-performance methods for the prediction of transmembrane helices.[25] The conservation of the two consensus NPA motifs in aquaporin sequences also helped to obtain trustworthy alignments. It is worth noting here that for membrane proteins it has been shown that sequence identity values required to derive accurate 3D models can be lower than those needed in the case of globular proteins.[26]

To test the reliability of our approach in predicting the structure of aquaporins at low sequence identity, we performed a blind prediction of the *Plasmodium falciparum* aquaglyceroporin (PfAQP) structure (see Supporting Information). PfAQP is a bifunctional aquaglyceroporin that efficiently allows the passage of both water and glycerol. Among the aquaporins of known structure, PfAQP is the one sharing the lowest sequence identity with the others. For the modeling procedure, we used six templates sharing with PfAQP a maximum sequence identity of 23% and not including any aquaglyceroporin (Supporting Information Fig. S1). Comparison with the experimental structure shows that the predicted model is substantially correct (Supporting Information Fig. S2). Pore-lining residues are correctly placed and most of their side chains accurately

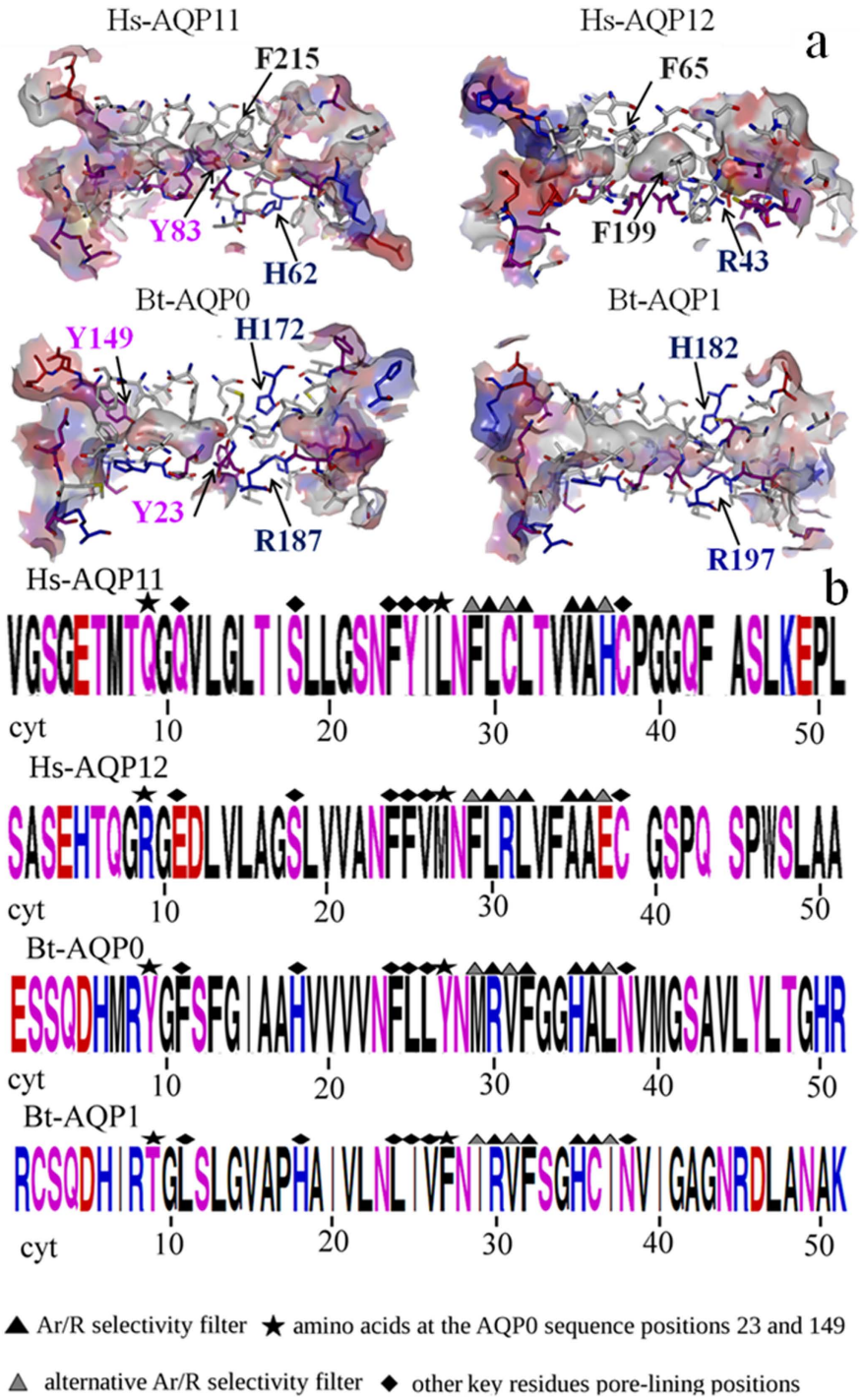

Figure 3. Representation of sequence and structural features of the pores. Each pore is orientated from the intracellular (left) to the extracellular (right) side. Acidic residues are colored in red, basic residues in blue, and polar residues in purple. (a) 3D-Structure representation: for h-AQP11, h-AQP12, Bt-AQP1 and Bt-AQP0, all the residues lining the pore are shown. (b) Sequence representation: pore-lining residues are shown as pore-logos for four AQPs. Note that logo numbers correspond to the structural position of the residues along the channel axis and not to their sequence position. Symbols are the same of Table I and Figure 1. [Color figure can be viewed in the online issue, which is available at wileyonlinelibrary.com.]

modeled. Deviations from the X-ray structure are only observed in extra-membrane loops. These findings suggest that a multitemplate approach to model the channel of aquaporins at low sequence identity can be considered safe. Moreover, they are in line with the well-known fact that the structure of aquaporins is particularly well conserved, despite the low sequence similarity shared by members of different subfamilies and their different transport functions. This observation is the result of the analysis and

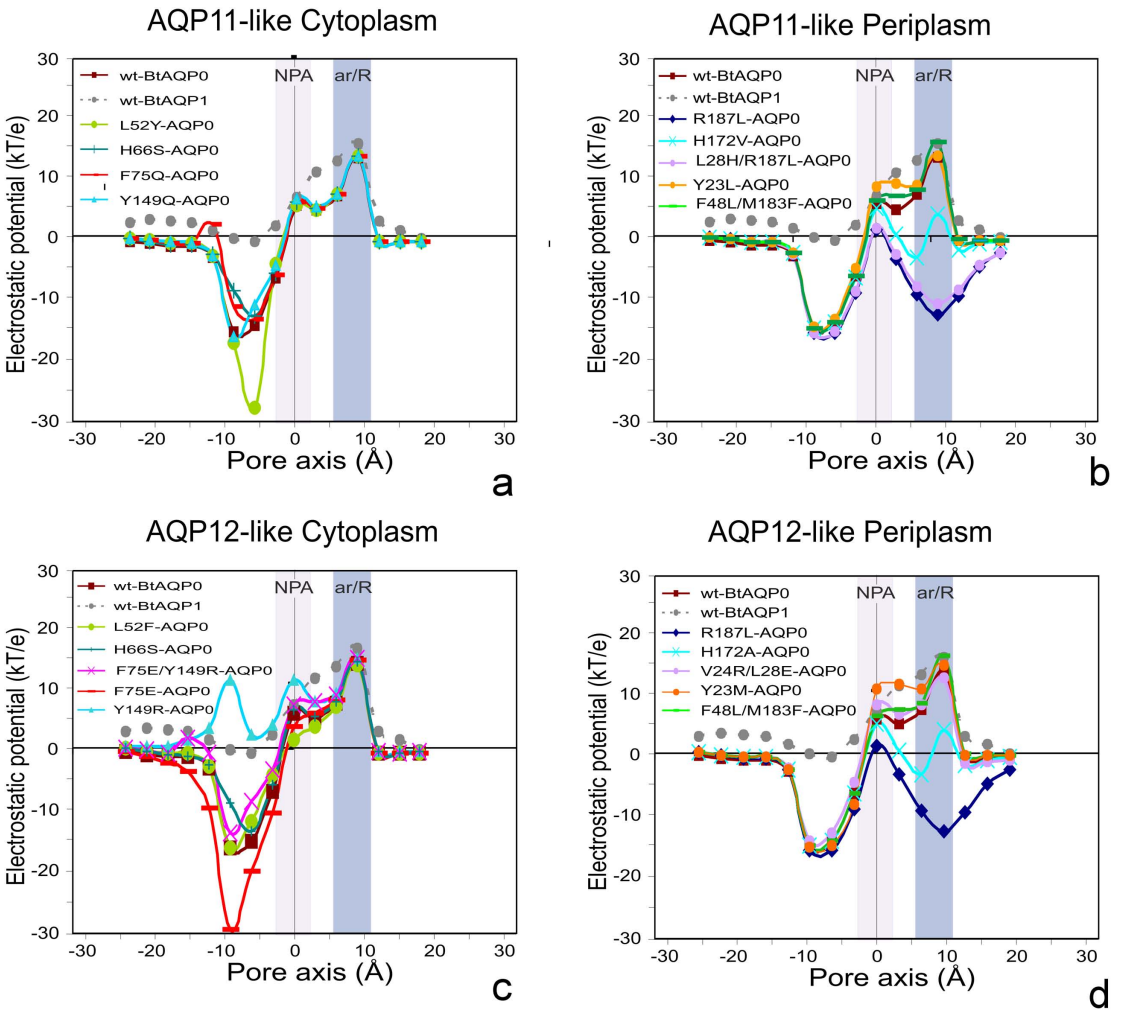

Figure 4. Electrostatic potential calculated at pore centers for BtAQP0 bearing: AQP11-like (top) and AQP12-like (bottom) substitutions. Electrostatic potentials are also shown for wt BtAQP0 and wt BtAQP1, for comparison. [Color figure can be viewed in the online issue, which is available at wileyonlinelibrary.com.]

comparison of 10 structures representative of different aquaporin subfamilies.[3,17]

Representations of the 3D models obtained for hAQP11 and hAQP12, emphasizing the pore shape and dimension, are given in Figure 3(a) for the obtained hAQP11 and hAQP12 models and for the crystallographic structures of BtAQP0[27] and of BtAQP1.[28]

Amino acid composition and physico-chemical properties of the pore

Ar/R selectivity filter (logo positions 30, 32, 35, 36 and 29, 31, 37). Both orthodox aquaporins and aquaglyceroporins have an ar/R constriction site, also known as selectivity filter, characterized by the presence of an arginine and an aromatic residue. The arginine is located immediately downstream of the C-terminal NPA motif (logo position 30) and is overall conserved among all known aquaporins. The only exceptions are plant TIP1 and SIP1, where it is substituted by a Val and an Asn, respectively, and mammalian AQP11 and AQP12, where it is substituted by a Leu219/203 (see Table I). Moreover, orthodox aquaporins, including AQP0, feature a characteristic ar/R aromatic Phe (logo position 32), which is substituted by a Trp in glycerol channels of known structure, and is a nonaromatic residue, Leu 79/61, in AQP11/AQP12. A third residue characterizing the constriction, which is a His in orthodox aquaporins (logo position 35), including AQP0, and a Gly in glycerol channels, in AQP11 and AQP12 is substituted by Val204 and Ala188, respectively. Finally, the fourth ar/R residue (logo position 36) is conserved, as compared to AQP0. It is indeed Ala213, Ala197, and Ala181 in AQP11, AQP12, and AQP0, respectively; in AQP1 instead the alanine is substituted by Cys191, having a role in the AQP1 mercurials sensitivity.

Therefore, AQP11 and AQP12 amino acids found at positions corresponding to the canonical aquaporin ar/R site, although giving a constriction, are completely hydrophobic in nature and lack both the characteristic aromatic and the basic residue. Which

Table I. *Identity of Residues at Key Pore-Lining Positions*

Logo position[a]	Pore height (Å)	hAQP11	hAQP12	hAQP0	hAQP1
9 ★	~ −12	Gln185	Arg169	Tyr149	Thr159
11 ◆	~ −12	Gln106	Glu88	Phe75	Leu85
18 ◆	~ −9	Ser97	Ser79	His66	His76
24 ◆	~ −3	Phe177	Phe161	Phe141	Leu151
25 ◆	~ −3	Tyr83	Phe65	Leu52	Ile62
26 ◆	~ 3	Ile200	Val184	Leu168	Val178
27 ★	~ 3	Leu57	Met42	Tyr23	Phe24
29 ▲	~ 3	Phe215	Phe199	Met183	Ile193
30 ▲	~ 3	Leu219	Leu203	Arg187	Arg197
31 ▲	~ 6	Cys58	Arg43	Val24	Val25
32 ▲	~ 6	Leu79	Leu61	Phe48	Phe58
35 ▲	~ 9	Val204	Ala188	His172	His182
36 ▲	~ 9	Ala213	Ala197	Ala181	Cys192
37 ▲	~ 9	His62	Glu47	Leu28	Ile29
38 ◆	~ 9/12	Cys155	Cys139	Asn119	Asn129

[a] Residues of the Ar/R selectivity filter and of the possible alternative Ar/R site are indicated with ▲ and ▲, respectively. Residues corresponding to the BtAQP0 sequence positions 23 and 149 are marked with ★. Other key pore-lining positions are pointed out with ◆.

is the effect of these substitutions on the functionality of AQP11 and AQP12? Beitz *et al*. experimentally showed that individual or joint mutations of the selectivity filter residues of hAQP1 lowered its selectivity.[29] In particular, the substitution of the Arg with a hydrophobic Val was unexpectedly shown to allow the passage of protons. On this bases, we previously performed an *in silico* analysis of Beitz's mutants and observed a dramatic change in the electrostatics of their channel. In particular, the Arg to Val mutation caused the periplasmic positive electrostatic trend to dramatically revert into negative.[17] One may wonder whether the substitution of these crucial pore-lining residues in AQP11 and AQP12 is still compatible with a selective transport of water.

Remarkably, we have observed that hAQP11 presents a basic residue, His62, at the periplasmic site of the channel (logo position 37) that is unique to this subfamily. Therefore, canonical aquaporins exhibit a pair of Arg and Leu residues at the logo positions 30 and 37, whereas AQP11 shows a pair of His and Leu residues at inverted sequence positions. hAQP12 also has a basic residue, Arg43, at the logo position 31, spatially close to the ar/R site, which is unique to this subfamily, as all other aquaporins exhibit a hydrophobic residue at such a position (Ile/Val/Leu/Met), with the exception of AQP11 having a cysteine. Interestingly, both AQP11 and AQP12 also present a pore-lining aromatic residue around the ar/R site (logo position 29), Phe215 in AQP11 and Phe199 in AQP12. Such Phe corresponds to smaller, hydrophobic residues like Ile/Val/Leu in other aquaporins. We suggest that the basic His62/Arg43 at the logo position 37/31 and the aromatic Phe215/Phe199 at the logo position 29 may represent a possible alternative Ar/R site for hAQP11 and hAQP12, respectively (but we remind that the logo positions 27 and 31 fall into the uncertain N-terminal region of the AQP12 alignment). This possible substitutive ar/R site is, however, wider than the canonical one and this explains the minor effect on the channel electrostatics of such basic residue (see below). At the logo position 37, AQP12 instead presents an acidic residue, Glu47, interestingly corresponding to PfAQP Glu125, which has been associated both experimentally and computationally to the peculiar nature of such aquaporin as a perfect bifunctional water and glycerol channel.[17,30]

We have calculated the electrostatic potential of *in silico* BtAQP0 mutants, where the above residues were substituted by the corresponding AQP11 and AQP12 ones. The electrostatic potentials of the BtAQP0 channel bearing AQP11 and AQP12-like mutations at its periplasmic side are shown in Figure 4, panels b and d, respectively. Mutating the BtAQP0 Phe48 to an AQP11/AQP12-like Leu has only minor effect on its electrostatics (data not shown). As expected, instead, the mutation of the ar/R arginine to a Leu causes a dramatic change similar to that observed for the analogous R197V mutation in hAQP1,[17] which results in the reversion of the positive trend to a negative one [see mutant R187L, Figure 4(b,d)].

Analogously, the mutation of the other basic residue of the ar/R site (His172 in AQP0, His182 in AQP1) to a Val/Ala, causes a decrease of the positive trend in the periplasmic half of the channel, by about 10 kT/e. These changes are only slightly counterbalanced by the mutation of BtAQP0 Leu28 to His62 in AQP11 (Supporting Information Fig. S3). In AQP12, Glu47 at the logo position 37 would further decrease the positive periplasmic trend, but its effect is compensated by the presence of the spatially close Arg43, at the logo position 31 (see mutant

V24R/L28E in Figure 4, panel d). As a consequence, the electrostatic profile of AQP11 and AQP12 channels, at the periplasmic side, is expected to be negative and to feature a quite deep minimum approximately at the height of the canonical ar/R site.

Role of amino acids at the AQP0 sequence positions 23 and 149 (logo positions 27 and 9). Several lines of evidence suggest that Tyr23 (logo position 27) and Tyr149 (logo position 9) may be associated to the low water conductance of bovine, and more generally of mammalian AQP0,[17,31,32] and that their mutation to the corresponding AQP1 residues, Phe and Thr, respectively, tends to restore dynamic and electrostatic features characteristic of orthodox aquaporins.[17,32] In particular, we have shown that Y149T and Y149F mutations tend to restore a flat orthodox-like trend at the cytoplasmic side of the channel, with the former substitution having a stronger effect. We have also shown that Tyr23 and Tyr149 are conserved among the low water conductance mammalian and amphibian AQP0s and are instead substituted by AQP1-like Phe and Thr residues, respectively, in high water conductance killifish AQP0, which features high water permeability.[33]

Interestingly, hAQP11 presents a Leu57 at the AQP0 position 23 and an unusual Gln185 at the AQP0 position 149 (Table I), both conserved within the AQP11 subfamily (see Supporting Information Fig. S4). Leu57 is smaller when compared with the corresponding AQP0 Tyr23 but also to the corresponding AQP1 Phe24. A leucine at such a position is indeed found in several glycerol channels, such as AQP3, AQP10, GlpF, and AQPM, (but also in the orthodox AqpZ), and should widen the pore. The BtAQP0 Y23L mutant exhibits an electrostatic profile shifted toward the canonical BtAQP1 profile at the periplasmic side of the channel immediately after the NPA region [Fig. 4(b)]. As for Gln185, it is really unusual; as such a residue gives less steric hindrance than the corresponding AQP0 Tyr149 and is not found in any other known aquaporin. The substitution of AQP0 Tyr149 with an AQP11-like Gln (mutant Y149Q) causes a slight alteration of the channel electrostatics with the profile moving by about 3.5 kT/e toward orthodox values, but only in a limited cytoplasmic region of the channel, close to the NPA motifs [Fig. 4(a)].

One of the above hAQP11 residues, Leu57, corresponding to mAQP0 Y23, has already been discussed, together with residue Tyr83 (logo position 25, see below) in the context of the low water conductance of AQP11.[13] It has indeed been outlined that at such positions the slow water permeable channels, mAQP0 and AQP11, share a pair of interchangeable tyrosine and leucine residues. However, such residues are not located at the same height of the pore and, consequently, we show here that their effect on the shape and electrostatics is experienced in different regions of the channel, on opposite sides of the NPA region (see Figs. 3 and 4).

In hAQP12, the AQP0 Tyr23 is substituted by Met42, but again it should be noted that this falls in an uncertain region of the alignment. Met42 gives less steric hindrance, when compared with a tyrosine, and causes a slight increase of the electrostatic profile between the ar/R and the NPA regions, toward canonical AQP1 values (see mutant Y23M in Fig. 4, panel d). Corresponding to the AQP0 Tyr149, hAQP12 presents instead a really unusual Arg169. These two residues give comparable steric hindrance but the mutation of the Tyr with a charged Arg, in this constriction region, causes a reversion of the cytoplasmic profile from negative to positive [Fig. 4(c)]. This change is however compensated by the mutation of AQP0 Phe75 to the AQP12 Glu88 (see below).

Other key pore-lining positions (logo positions 11, 18, 24, 25 and 26). In addition to the above widely investigated pore-lining residues, we had also previously outlined the role of other amino acids in discriminating the pore features of AQP0s exhibiting different water permeabilities, that is, the low-water conductance mammalian AQP0 and the high-water permeability killifish AQP0. Such amino acids are located at sequence positions 75, 141, 52, and 168, as referred to bovine AQP0 [corresponding to logo positions 11, 24, 25, and 26, respectively, Table I and Fig. 3(b)]. Interestingly, such positions can also be used to describe peculiar hAQP11 and hAQP12 pore features. In particular, BtAQP0 Phe75, Phe141, Leu52, and Leu168 are substituted by Gln106, Phe177, Tyr83, and Ile200 in hAQP11, and Glu88, Phe161, Phe65, and Val184 in hAQP12, respectively. All these residues are conserved within the two subfamilies (Fig. S4).

As for hAQP11, Gln106 is unique among human aquaporins and is not found in any other known aquaporin. Analogously to Gln185, it is less bulky than the corresponding Phe75 AQP0 residue. Moreover, the F75Q mutation in BtAQP0 also causes an alteration of the channel electrostatics toward orthodox values in a limited region that is further shifted toward the cytoplasm, when compared with the above Y149Q mutant [Fig. 4(a)].

Phe177 of AQP11 is conserved when compared with mammalian AQP0 and substitutes a Leu in fish AQP0 and in AQP1. This residue gives a steric hindrance that might therefore be associated to the low water transport efficiency of both AQP11 and mammalian AQP0. Tyr83 substitutes a Leu/Ala in AQP0 (a Phe in only 2 cases) and an Ile in AQP1, whereas Ile200 corresponds to a Leu and a Val in AQP0 and AQP1, respectively. Therefore, Ile200 and

especially Tyr83, contribute to narrow the region of the hAQP11 channel they are located in, when compared with the corresponding AQP0 and AQP1 residues. In our AQP11 3D model, the Tyr83 side chain occupies a pore-lining region nearby to that occupied by the Tyr23 side chain in AQP0 (see previous subsection). A tyrosine lining the pore is expected, analogously to the AQP0 Tyr23, to significantly influence the channel electrostatics.[20] Indeed, the channel electrostatics of the L52Y BtAQP0 mutant shows a dramatically deepened minimum at the cytoplasmic side that accentuates the nonorthodox character of the native mammalian AQP0 profile [Fig. 4(a)].

As for AQP12, Glu88 is as well unique among human aquaporins and not found in any other known aquaporin. Analogously to AQP11 Gln106, it gives less steric hindrance than the corresponding mAQP0 residue but has a dramatic effect on the electrostatics of the channel, significantly deepening the minimum at the cytoplasmic side [F75E BtAQP0 mutant, Fig. 4(c)]. Phe161 corresponds to hAQP11 Phe177 and BtAQP0 Phe141 and might therefore be associated to a low or impaired water transport in AQP12. Phe65, similarly to hAQP11 Tyr83, contribute to locally narrow the diameter of the AQP12 channel, when compared with both the AQP0 Leu52 and the AQP1 Ile62 (by about 2 Å), but it has only marginal effects on the channel electrostatics [see mutant L52F in Fig. 4(c)].

It is also very interesting that both AQP11 and AQP12 present a Ser (Ser97 and Ser79, respectively) instead of BtAQP0 His66 (logo position 18), which is conserved in all aquaporins except for the poorly characterized SIP1, where it is also a Ser. A Ser in this position should contribute to widen the pore. In addition, it does influence the electrostatics causing a shift of the curve toward a flat orthodox profile in a limited region at the cytoplasmic side of the channel, as shown by the electrostatic profile of the H66S BtAQP0 mutant shown in Fig. 4(a,c).

To summarize the results of the electrostatic calculations on the substitutions at the cytoplasmic side of the channels, the AQP11-like L52Y and AQP12-like F75E mutants have a dramatic effect on the native BtAQP0 channel electrostatics, further deepening the AQP0 typical cytoplasmic minimum [Fig. 4(a,c)]. As for the other substitutions (Y149Q, F75Q, H66S in hAQP11 and L52F, H66S in hAQP12), they all show only a minor effect, slightly tending to restore an orthodox-like trend. Interestingly, the AQP12-like Y149R mutant is instead able to reverse the profile from negative to positive. However, its effect is compensated by that of the above mentioned F75E mutant [see the double mutant F75E/Y149R, in Fig. 4(c)]. Therefore, also at the cytoplasmic side of the channel, the electrostatic profile for both AQP11 and AQP12 is expected to be negative, with a probably deepened minimum as compared to BtAQP0.

Cysteine residues

AQP11 cysteines deserve a special mention. Indeed, the AQP11 subfamily is particularly rich in cysteines, with 10 cysteine residues, whose role remains to be clarified. One of these, Cys101, occupies the third position of the N-terminal consensus motif, resulting in a NPC instead of a NPA sequence. It has been shown that the substitution of this cysteine with a canonical alanine reduces the AQP11 water transport efficiency, pointing to a functional role that needs to be further investigated.[34] In addition, it has been shown that AQP11 needs the NPC motif to form tetramers.[34] Thus, it has been suggested that mutations at the AQP11 unique Cys may interfere with the folding of individual subunit, leading to misalignment of surrounding contact points between monomers. In our hAQP11 3D model, the Ala to Cys substitution within one of the NPA motifs seems to be responsible for neither global nor local conformation peculiarities as compared to other aquaporins. Cys101 in the AQP11 3D model is, as expected, located within the pore and does not give any contact with residues from other monomers. This is not surprising, as we know the 3D-structure at 2.05 Å resolution of the *Plasmodium falciparum* aquaporin (PfAQP), which exhibits two unusual NPA motifs: NLA and NPS, at the N-terminal and C-terminal side, respectively. The PfAQP overall conformation and its local conformation around the NPA region presents no striking difference with respect to the other aquaporins of known 3D-structure.[35] The role of Cys101 in determining the hAQP11 mercurial sensitivity has also been investigated and no significant inhibition has been found.[13] However, two other cysteines occupy pore-lining positions: Cys58 (logo position 31) and Cys155 (logo position 38). Cys58 is absolutely unique to this subfamily, whereas Cys155 is also found in AQP12 (see below). The possible binding of mercurials to these two cysteines is therefore worth to be further investigated.

In addition, a point mutation to serine of a conserved cysteine, nine residues downstream of the C-terminal NPA motif (Cys227 in AQP11 and Cys211 in AQP12), was reported to produce a phenotype similar to that of AQP11-null mice.[15] In our 3D models of the AQP11 and AQP12 tetramers, this cysteine is exposed on the surface of the protein, at the periplasmic side of the membrane.

As for AQP12, it presents six cysteine residues, Cys139 being pore-exposed (logo position 38) and having a possible role in the mercurials sensitivity that could be experimentally investigated. It also worth noting that from a structural point of view, Cys211 in AQP12 is perfectly equivalent to Cys227 in AQP11. Therefore, it would also be worth investigating the possible functional role of this residue.

Conserved residues

The alignment of superaquaporins AQP11 and AQP12 to their paralogs, notwithstanding the low overall sequence identity, highlights the strict conservation of few amino acids (see consensus sequences in Figs. 1 and 2). Referring to the BtAQP0 numbering, conserved amino acids, besides Asn68 and Asn184-Pro185 within the aquaporin characterizing NPA motifs, are: Glu16, Gly64, Gln93, Glu134, Pro208, and Gly211.

Such residues clearly have a structural role and indeed they include three "special" residues from a structural point of view, that is, two glycines and one proline. Among these, Gly64 (Gly95/77 in hAQP11/hAQP12), located in loop B four residues upstream of the N-terminal NPA, assumes values of ϕ and Ψ angles (130° and −24°, respectively) not accessible to other amino acids. Further, conserved residues include two glutamic acids (Glu50/35, and Glu170/154, respectively, in hAQP11/hAQP12) whose role in anchoring the position of transmembrane helices 1 and 4 relative to the functional loops B and E, through H-bonding with residues immediately upstream of the NPA motifs, has long been established.[36] The conserved glutamine (Gln124/106 in hAQP11/hAQP12) is also involved, together with Glu16, in the H-bond network around the N-terminal NPA region.

Interestingly, such residues seem to define a minimal set of structural requirements for the maintenance of the correct aquaporins scaffold, independently from their transport efficiency and specificity.

Methods

Model building and analysis

Human AQP11 and AQP12 sequences were collected from the SwissProt database.[37] In the manually reviewed UniProtKB/Swiss-Prot dataset, two entries are available for human AQP12, corresponding to the two AQP12A and AQP12B genes (ID: Q8FXI and A6NM10, respectively). Although hAQP12B is reported to present isoforms 1 and 2, the isoform-1 has been chosen as "canonical" sequence from the Swiss-Prot reviewers, as for the isoform-2 no experimental information is available. hAQP12A and hAQP12B-isoform-1 sequences are 99% identical, with only three substitutions in non-pore-lining positions; therefore, for the sake of clarity, in the following only the hAQP12A sequence will be presented and discussed. Comparative models were built with Modeler,[38] using a multitemplate approach. Ten structures, each of them representative of a different aquaporin subfamily, were used as templates (AQP0, PDBcode: 1ymg; AQP5, PDBcode:3d9s; AQP4, PDBcode:3gd8; AQP1, PDBcode:1j4n; AQPM, PDBcode:2f2b; AQY1, PDBcode:2w2e; GlpF, PDBcode:1ldf; PfAQP, 3c02; SoPIP2, PDBcode:3cn5; AQPZ2, PDBcode:3llq). Sequence alignments for the modeling procedure were obtained by HHPred,[24] and cross-checked with the prediction of the transmembrane helices as obtained by MEMSAT-SVM.[25] The hAQP12 alignment was manually adjusted to have the first transmembrane helix correctly aligned between the structural templates. The sequence identities with the templates were in the range 13%–19% for hAQP11 and from 15 to 19% for hAQP12. The models quality was tested by ProQ,[39] finding LG-scores of 2.47 and 2.00 for the hAQP11 and the hAQP12 model, respectively, and by Qmean,[40] finding total scores of 0.487 (Z-score: −3.06) and of 0.397 (*Z*-score: −4.03). The sequence correspondence between hAQP11/hAQP12 and BtAQP0 was used to compare them to a comprehensive set of 220 nonfragment aquaporin sequences, previously collected from the Uniprot Knowledge database (see Ref. 17 for details) and aligned with HMMER.[41]

hAQP11 and hAQP12 pore-logos were derived from the 51 sequence alignment positions previously identified as pore-lining positions of the aquaporin family, as detailed in Ref. 17. Sequence logos of the pore-lining residues were obtained by the PoreLogo web tool.[18] The BtAQP0 Y23L, Y23M, V24R, V24R/L28E, F48L, L52Y, L52F, H66S, F75Q, F75E, Y149Q, and H66T and F75Q and Y149Q L28H/R187L, R187L, F48L/M183F, F75E/Y149R mutants were modeled by the Modeler selection-mutate procedure. The channel electrostatic potential of the BtAQP0 mutants was calculated by solving the Poisson–Boltzmann equation using the APBS program,[42] as detailed in Ref. 17.

Conclusions

3D models have been obtained for hAQP11 and hAQP12 using all the available structural information and state-of-art techniques. Sequences of the two superaquaporins appear to be perfectly compatible with both the tertiary and quaternary arrangement shared by the 10 aquaporin subfamilies of known 3D-structure. However, their channels appear to be quite narrow, especially that of hAQP12, presenting one constriction at the cytoplasmic and one at the periplasmic side. This is the consequence of amino acids substitution at key pore-lining positions. In the central region of the channel the two superaquaporins present peculiar bulge aromatic residues, such as Tyr83/Phe65 and Phe215/Phe199 causing a significant narrowing of the pore. In addition, hAQP12 hosts a Met42, corresponding to the mAQP0 Tyr23, and a Phe198 (logo position 34) at the periplasmic side of the NPA region.

Composition of the hAQP11 and hAQP12 channels is quite anomalous, having a less basic character than the canonical AQP0 and AQP1 ones. Indeed three basic residues (at logo positions 18, 30 and 35),

two of them belonging to the ar/R site, are missing, substituted by polar or hydrophobic residues. However, one peculiar basic residue is observed in hAQP11, His62, and one in hAQP12, Arg43, that we suggest to possibly play a role as an alternative ar/R site in such aquaporins, together with the aromatic residue, Phe215/199. In addition, the hAQP12 channel presents three peculiar acidic residues in its inner region (logo positions 11, 12, and 37), thus assuming an unusual acidic character. We have shown that all these amino acid substitutions, involving charged amino acids, can dramatically influence the electrostatics of the channels, resulting in an unusual double-humped negative profile.

On these bases, we conclude that several factors are expected to hamper the water transport in hAQP11 and hAQP12. Among these, the narrowing of the channels, their anomalous electrostatic profile and the lack of a canonical ar/R site, although maybe compensated by the presence of a possible alternative ar/R site that we identified approximately at the same height of the pore. As for hAQP12, its pore shape and anomalous composition may constitute an additional obstacle to the water passage.

Obviously many aspects concerning the molecular and biological function of hAQP11 and hAQP12 remain to be clarified and experiments are expected to provide conclusive answers to many questions, which are still open. However, we believe that in this scenario the results of this study may constitute the basis for the design of novel dedicated experiments to provide additional contributions and illuminate the functional role of these unique aquaporins.

References

1. Zardoya R (2005) Phylogeny and evolution of the major intrinsic protein family. Biol Cell 97: 397–414.
2. Gomes D, Agasse A, Thiebaud P, Delrot S, Geros H, Chaumont F (2009) Aquaporins are multifunctional water and solute transporters highly divergent in living organisms. Biochim Biophys Acta 1788: 1213–1228.
3. Gonen T, Walz T (2006) The structure of aquaporins. Q Rev Biophys 39: 361–396.
4. Wang Y, Schulten K, Tajkhorshid E (2005) What makes an aquaporin a glycerol channel? A comparative study of AqpZ and GlpF. Structure 13: 1107–1118.
5. Ishibashi K, Hara S, Kondo S (2009) Aquaporin water channels in mammals. Clin Exp Nephrol 13: 107–117.
6. Morishita Y, Sakube Y, Sasaki S, Ishibashi K (2004) Molecular mechanisms and drug development in aquaporin water channel diseases: aquaporin superfamily (superaquaporins): expansion of aquaporins restricted to multicellular organisms. J Pharmacol Sci 96: 276–279.
7. Yakata K, Hiroaki Y, Ishibashi K, Sohara E, Sasaki S, Mitsuoka K, Fujiyoshi Y (2007) Aquaporin-11 containing a divergent NPA motif has normal water channel activity. Biochim Biophys Acta 1768: 688–693.
8. Itoh T, Rai T, Kuwahara M, Ko SB, Uchida S, Sasaki S, Ishibashi K (2005) Identification of a novel aquaporin, AQP12, expressed in pancreatic acinar cells. Biochem Biophys Res Commun 330: 832–838.
9. Ohta E, Itoh T, Nemoto T, Kumagai J, Ko SB, et al. (2009) Pancreas-specific aquaporin 12 null mice showed increased susceptibility to caerulein-induced acute pancreatitis. Am J Physiol Cell Physiol 297: C1368–1378.
10. Morishita Y, Matsuzaki T, Hara-chikuma M, Andoo A, Shimono M, et al. (2005) Disruption of aquaporin-11 produces polycystic kidneys following vacuolization of the proximal tubule. Mol Cell Biol 25: 7770–7779.
11. Gorelick DA, Praetorius J, Tsunenari T, Nielsen S, Agre P (2006) Aquaporin-11: a channel protein lacking apparent transport function expressed in brain. BMC Biochem 7: 14.
12. Magni F, Sarto C, Ticozzi D, Soldi M, Bosso N, Mocarelli P, Kienle MG (2006) Proteomic knowledge of human aquaporins. Proteomics 6: 5637–5649.
13. Yakata K, Tani K, Fujiyoshi Y (2011) Water permeability and characterization of aquaporin-11. J Struct Biol 174: 315–320.
14. Finn RD, Clements J, Eddy SR (2011) HMMER web server: interactive sequence similarity searching. Nucleic Acids Res 39: W29–W37.
15. Tchekneva EE, Khuchua Z, Davis LS, Kadkina V, Dunn SR, et al. (2008) Single amino acid substitution in aquaporin 11 causes renal failure. J Am Soc Nephrol 19: 1955–1964.
16. Gonen T, Cheng Y, Sliz P, Hiroaki Y, Fujiyoshi Y, Harrison SC, Walz T (2005) Lipid-protein interactions in double-layered two-dimensional AQP0 crystals. Nature 438: 633–638.
17. Oliva R, Calamita G, Thornton JM, Pellegrini-Calace M (2010) Electrostatics of aquaporin and aquaglyceroporin channels correlates with their transport selectivity. Proc Natl Acad Sci USA 107: 4135–4140.
18. Oliva R, Thornton JM, Pellegrini-Calace M (2009) PoreLogo: a new tool to analyse, visualize and compare channels in transmembrane proteins. Bioinformatics 25: 3183–3184.
19. Pellegrini-Calace M, Maiwald T, Thornton JM (2009) PoreWalker: a novel tool for the identification and characterization of channels in transmembrane proteins from their three-dimensional structure. PLoS Comput Biol 5: e1000440.
20. Calvanese L, Pellegrini-Calace M, Oliva R (2010) Mutations at key pore-lining positions differentiate the water permeability of fish lens aquaporin from other vertebrates. FEBS Lett 584: 4797–4801.
21. de Groot BL, Grubmuller H (2001) Water permeation across biological membranes: mechanism and dynamics of aquaporin-1 and GlpF. Science 294: 2353–2357.
22. Tajkhorshid E, Nollert P, Jensen MO, Miercke LJW, O'Connell J, Stroud RM, Schulten K (2002) Control of the selectivity of the aquaporin water channel family by global orientational tuning. Science 296: 525–530.
23. Mariani V, Kiefer F, Schmidt T, Haas J, Schwede T (2011) Assessment of template based protein structure predictions in CASP9. Proteins 79 Suppl 10: 37–58.
24. Soding J, Biegert A, Lupas AN (2005) The HHpred interactive server for protein homology detection and structure prediction. Nucleic Acids Res 33: W244–W248.
25. Nugent T, Jones DT (2010) Predicting transmembrane helix packing arrangements using residue contacts and a force-directed algorithm. PLoS Comput Biol 6: e1000714.
26. Forrest LR, Tang CL, Honig B (2006) On the accuracy of homology modeling and sequence alignment methods applied to membrane proteins. Biophys J 91: 508–517.

27. Harries WE, Akhavan D, Miercke LJ, Khademi S, Stroud RM (2004) The channel architecture of aquaporin 0 at a 2.2-A resolution. Proc Natl Acad Sci USA 101: 14045–14050.
28. Sui H, Han BG, Lee JK, Walian P, Jap BK (2001) Structural basis of water-specific transport through the AQP1 water channel. Nature 414: 872–878.
29. Beitz E, Wu B, Holm LM, Schultz JE, Zeuthen T (2006) Point mutations in the aromatic/arginine region in aquaporin 1 allow passage of urea, glycerol, ammonia, and protons. Proc Natl Acad Sci USA 103: 269–274.
30. Beitz E, Pavlovic-Djuranovic S, Yasui M, Agre P, Schultz JE (2004) Molecular dissection of water and glycerol permeability of the aquaglyceroporin from Plasmodium falciparum by mutational analysis. Proc Natl Acad Sci USA 101: 1153–1158.
31. Jensen MO, Dror RO, Xu H, Borhani DW, Arkin IT, Eastwood MP, Shaw DE (2008) Dynamic control of slow water transport by aquaporin 0: implications for hydration and junction stability in the eye lens. Proc Natl Acad Sci USA 105: 14430–14435.
32. Qiu H, Ma S, Shen R, Guo W (2010) Dynamic and energetic mechanisms for the distinct permeation rate in AQP1 and AQP0. Biochim Biophys Acta 1798: 318–326.
33. Virkki LV, Cooper GJ, Boron WF (2001) Cloning and functional expression of an MIP (AQP0) homolog from killifish (Fundulus heteroclitus) lens. Am J Physiol Regul Integr Comp Physiol 281: R1994–R2003.
34. Ikeda M, Andoo A, Shimono M, Takamatsu N, Taki A, et al. (2011) The NPC motif of aquaporin-11, unlike the NPA motif of known aquaporins, is essential for full expression of molecular function. J Biol Chem 286: 3342–3350.
35. Newby ZER, O'Connell J, 3rd, Robles-Colmenares Y, Khademi S, Miercke LJ, Stroud RM (2008) Crystal structure of the aquaglyceroporin PfAQP from the malarial parasite Plasmodium falciparum. Nat Struct Mol Biol 15: 619–625.
36. Murata K, Mitsuoka K, Hirai T, Walz T, Agre P, Heymann JB, Engel A, Fujiyoshi Y (2000) Structural determinants of water permeation through aquaporin-1. Nature 407: 599–605.
37. Apweiler R, Bairoch A, Wu CH, Barker WC, Boeckmann B, et al. (2004) UniProt: the Universal Protein knowledgebase. Nucleic Acids Res 32: D115–D119.
38. Sali A, Blundell TL (1993) Comparative protein modelling by satisfaction of spatial restraints. J Mol Biol 234: 779–815.
39. Wallner B, Elofsson A (2006) Identification of correct regions in protein models using structural, alignment, and consensus information. Protein Sci 15: 900–913.
40. Benkert P, Kunzli M, Schwede T (2009) QMEAN server for protein model quality estimation. Nucleic Acids Res 37: W510–W514.
41. Eddy SR (2009) A new generation of homology search tools based on probabilistic inference. Genome Inform 23: 205–211.
42. Baker NA, Sept D, Joseph S, Holst MJ, McCammon JA (2001) Electrostatics of nanosystems: application to microtubules and the ribosome. Proc Natl Acad Sci USA 98: 10037–10041.